

ANL/CHM/CP--92452

CONF-961040--23

IN SITU Fe K-EDGE X-RAY ABSORPTION FINE STRUCTURE OF A PYRITE
ELECTRODE IN A Li/POLYETHYLENE OXIDE(LiClO₄)/FeS₂ BATTERY ENVIRONMENT

Dana Totir,⁺ In Tae Bae,⁺ Yining Hu,⁺ Mark R. Antonio,⁺⁺ and
Daniel A. Scherson⁺

⁺ Department of Chemistry
Case Western Reserve University
Cleveland, OHIO 44106-7078

⁺⁺ Chemistry Division
Argonne National Laboratory
9700 South Cass Avenue
Argonne, IL 60439-4837

RECEIVED

MAR 25 1997

OSTI

Electronic and structural properties of materials generated by the reduction and subsequent oxidation of pyrite in a lithium-based solid polymer electrolyte have been examined by *in situ* fluorescence Fe K-edge X-ray absorption fine structure (XAFS) in a FeS₂/Li battery environment. The XAFS results obtained are consistent with the formation of metallic iron as one of the products of the full (4-electron) discharge, in agreement with information reported in other laboratories. Extended X-ray absorption fine structure (EXAFS) data reveal that a subsequent 2-electron or 4-electron recharge generates a species with a Fe-S bond distance identical to that of pyrite, $d(\text{Fe-S}) = 2.259 \text{ \AA}$, with no other clearly detectable interactions due to more distant atoms. Based on the similarities between the metrical parameters and other features in the X-ray absorption near edge structure (XANES), the ferrous sites in these species appear to be tetrahedrally coordinated, as in chalcopyrite (CuFeS₂), for which $d(\text{Fe-S})$ is 2.257 \AA , and, thus, different than in Li₂FeS₂, a material that exhibits longer Fe-S distances.

INTRODUCTION DISTRIBUTION OF THIS DOCUMENT IS UNLIMITED

The electrochemical reactivity of pyrite in non-aqueous, lithium-based electrolytes continues to receive attention from both scientific¹⁻⁵ and industrial⁶ communities. Much of the impetus for research in this area is derived from the prospects of developing high energy density, low cost, and environmentally safe rechargeable Li/FeS₂ batteries with potential use in vehicular propulsion and other applications. A number of structural and spectroscopic techniques, including *in situ* X-ray diffraction (XRD),² *in situ* ⁵⁷Fe Mossbauer effect spectroscopy (MES)^{2,3} and *in situ* X-ray absorption fine structure (XAFS)⁵ have been employed to establish the identity of cell

The submitted manuscript has been authored by a contractor of the U. S. Government under contract No. W-31-109-ENG-38. Accordingly, the U. S. Government retains a nonexclusive, royalty-free license to publish or reproduce the published form of this contribution, or allow others to do so, for U. S. Government purposes.

MASTER

DISCLAIMER

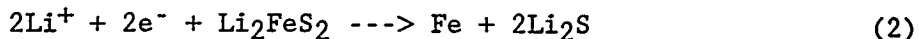
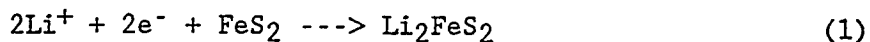
This report was prepared as an account of work sponsored by an agency of the United States Government. Neither the United States Government nor any agency thereof, nor any of their employees, make any warranty, express or implied, or assumes any legal liability or responsibility for the accuracy, completeness, or usefulness of any information, apparatus, product, or process disclosed, or represents that its use would not infringe privately owned rights. Reference herein to any specific commercial product, process, or service by trade name, trademark, manufacturer, or otherwise does not necessarily constitute or imply its endorsement, recommendation, or favoring by the United States Government or any agency thereof. The views and opinions of authors expressed herein do not necessarily state or reflect those of the United States Government or any agency thereof.

DISCLAIMER

Portions of this document may be illegible in electronic image products. Images are produced from the best available original document.

reaction products and determine the factors that control the extent of reversibility.

In particular, Dahn and coworkers, based on *in situ* XRD² and *in situ* ⁵⁷Fe MES data^{2,3} obtained for FeS₂ electrodes in a non-aqueous liquid electrolyte concluded that at high temperatures (> 37°C), or sufficiently low discharge rates at lower temperatures (21 - 30°C), the discharge curves of Li/FeS₂ cells display two plateaus associated with the step-wise reduction of pyrite to form Li₂FeS₂ as an intermediate, i.e.



Although Fe and Li₂S could be positively identified in the *in situ* XRD pattern of cells that had been discharged to the equivalent to three equivalents of Li per Fe (Li/Fe), no evidence could be obtained from this technique for the presence of Li₂FeS₂, leading these authors to suggest that this electrochemically formed material was amorphous (am.) when generated at these temperatures. Support for this view was gained from the close resemblance of the recharge profiles (Voltage vs Li/Fe ratio) of Li/FeS₂ cells, which had been discharged to 2 Li/Fe, and charge (lithium insertion) profiles of Li/Li₂FeS₂ cells prepared with chemically synthesized crystalline Li₂FeS₂ (cryst.) up to 2Li/Fe equivalent.

The recharge of a 4 Li/Fe discharged Li/FeS₂ cell was characterized by a plateau at 1.7 V ascribed to the reverse of Eq.(2) above, up to 2 Li/Fe, regenerating Li₂FeS₂(am.). Additional *in situ* XRD experiments involving Li/Li₂FeS₂(cryst.) cells² revealed that up to 40%, Li⁺ could be reversibly removed from the Li₂FeS₂ lattice for more than 60 cycles. Regardless of whether the electrode was 2 Li/Fe or 4 Li/Fe discharged FeS₂ or Li₂FeS₂(cryst.), the subsequent full removal of Li⁺ in the temperature range examined did not lead to the formation of FeS₂. This behavior is unlike that observed for Li/FeS₂ batteries at higher temperatures (T = 400°C) in a molten salt electrolyte,⁴ for which FeS₂(cubic) is indeed reformed upon full recharge, independent of the extent of prior discharge.

This work presents *in situ* fluorescence Fe K-edge X-ray absorption fine structure (XAFS) data for a FeS₂ cathode in a Li/FeS₂ solid polymer electrolyte battery operating at 55°C at various stages of discharge and recharge to gain insight into the nature of the intermediate species denoted as Li₂FeS₂(am.). In contrast to earlier studies involving *in situ* XAFS measurements on an operating Li/FeS₂ battery in a liquid, lithium-based electrolyte involving rather thick technical-type FeS₂ electrodes,⁵ the data shown herein is virtually free from thickness effects, thereby enabling a more detailed analysis of the X-ray absorption near edge structure (XANES).

EXPERIMENTAL

All operations involved in the preparation of components and overall cell assembly, including film casting and curing, FeS₂ grinding, cell sealing, and packaging in Ar-filled containers for shipment, were performed in a high quality glove box equipped with an O₂ sensor, under a high purity Ar atmosphere (O₂ < 3 ppm). Additional monitoring of the overall purity of the Ar in the glove box was provided by exposing freshly scraped lithium strips and checking visually for any losses in brightness.

A schematic diagram of the Li/FeS₂ cell designed for *in situ* Fe-K-edge XAFS studies in the fluorescence mode is shown in Panel A, Fig. 1. This battery-type, sandwich arrangement, is built around a LiClO₄-doped poly(ethylene oxide) (PEO) solid polymer electrolyte (10 mm x 8 mm, 35 μm thick) prepared by methods described elsewhere.⁷ The cathode is formed by spreading ca. 0.1 mg of freshly ground pyrite onto a rectangular section of the PEO(LiClO₄) film (0.32 cm²). A piece of gold-sputtered Ni foil placed directly above the cathode serves as a current collector. To complete the cell, a thin Li strip 0.5 mm thick, used as a counter-reference [C/R] electrode, is attached to the other side of the PEO(LiClO₄) film. To isolate the cell from the ambient atmosphere, the whole assembly, except for thin Ni wires that allow external connection to each of the electrodes, is encased in a heat-sealed polyethylene bag. Freshly assembled FeS₂/PEO(LiClO₄)/Li cells yielded stable open circuit potentials of ca. 3 V.

Based on the amount of pyrite and the size of the cathode, the attenuation at the Fe K-edge, assuming an absorption cross section of 380 cm²/g amounts to 1/20 absorption lengths. An analysis of AFM images (Nanoscope II, Digital Instruments) of the dispersed cathode on PEO/LiClO₄ acquired in air (see Panel A, Fig. 2) yielded an ensemble of evenly distributed particles of average dimensions on the order of only 1 μm. These features may be attributed to pyrite, as images of bare PEO(LiClO₄) surfaces obtained under the same conditions were found to be virtually featureless (see Panel B, Fig. 2), except for occasional strands (1 μm long, 0.3 μm diameter) ascribed to the structure of the polymer electrolyte itself. Based on the number of absorption lengths (0.05) and the average particle size (ca. 1 μm), self-absorption effects may be expected to be negligible; hence, the X-ray absorption near edge structure (XANES) features obtained in fluorescence can be assumed to be virtually undistorted. In fact, essentially no differences could be found between data collected *in situ* in fluorescence for a fresh cell and *ex situ* in transmission under ideal conditions (ca. 1 absorption length). This represents a significant improvement over our earlier *in situ* transmission Fe-K-edge XAFS of the FeS₂/Li system in a liquid non-aqueous solvent electrolyte performed with much thicker FeS₂ *technical* electrodes,⁵ which yielded highly distorted *in situ* XANES data.

During electrochemical experiments, the cells were placed on a U-shaped copper holder (see Panel B, Fig. 1) and held under pressure using a removable Al block/Al bar assembly. The temperature was maintained at a constant value, usually $55 \pm 0.5^\circ\text{C}$ by means of a heater/thermocouple (TC) arrangement connected to an Omega CN9000 controller. For the purely electrochemical characterization, voltammetric scans were performed at $70 \mu\text{V}/\text{s}$, whereas for the *in situ* XAFS measurements, each state of discharge and recharge was achieved by scanning the potential of the FeS_2 electrode linearly at $250 \mu\text{V}/\text{s}$ to the desired value. Once the prescribed state of charge had been reached, the Al block in front of the cell was removed to expose the cell to the x-ray beam at the operating temperature.

In situ XAFS data were acquired at the Stanford Synchrotron Radiation Laboratory (SSRL, line 4-1) with ring currents in the range of 40 to 100 mA at 3 GeV, using a set of two Si(111) crystals to monochromatize the radiation in the energy range of interest. Harmonic contributions were rejected by detuning the primary beam to 50% of its original intensity. All spectra were recorded in the fluorescence mode using a Lytle-type fluorescence detector (EXAFS Co., Pioche, NV) with a Mn filter (3 absorption lengths thick) placed between the sample and the detector. The Fe K-edge energy (Fe_{edge}) was calibrated using the first inflection point of the XANES of an Fe foil recorded in the transmission mode after each fill ($\text{Fe}_{\text{edge}} = 7112 \text{ eV}$). The X-ray energy was scanned with respect to the Fe_{edge} in the range -200 to -50 eV for the pre-edge region, and -50 to +70 eV for the XANES region in increments of 2 and 0.35 eV, respectively, and in steps of 0.05 \AA^{-1} for the EXAFS region, up to 975 eV (vs Fe_{edge}).

The analysis of the EXAFS data was performed using EXAFSPAK, a special set of routines developed by I. Pickering and G. George at SSRL.⁸ Fourier transforms (FT) of the k^3 -multiplied reduced EXAFS function ($k^3\chi(k)$) were obtained over the range $3.0 - 11.5 \text{ \AA}^{-1}$ ($\Delta k = 8.5 \text{ \AA}^{-1}$) without phase correction. The prominent Fe-S shell in the resulting radial distribution function was back-Fourier transformed using a window of 0.7 to 3.7 \AA ($\Delta r = 3.0 \text{ \AA}$). Theoretical phase and amplitude data obtained from FEFF⁹ (version 5.05) were used for fitting the filtered EXAFS functions.

RESULTS

Electrochemistry

The cyclic voltammogram of a FeS_2 electrode recorded at $70 \mu\text{V}/\text{s}$ in a cell identical to that used for *in situ* XAFS experiments at 55°C initiated at the open circuit potential yielded, in the first scan in the negative direction, a negligible current down to ca. 1.6 V vs. Li[C/R], followed by a clearly-defined peak at more negative potentials (see curve A, Fig. 3). In contrast, two prominent features, centered at 1.75 (A') and 2.4 V (B'), were found upon reversing the scan at 0.9 V as shown in the same Panel. During the second, and subsequent cycles (see curve b, Fig. 3), however, the voltammograms were characterized by

two peaks in the negative scan centered at 2 V (B) and 1.4 V (A), and the same features (except for slight shifts in the peak potentials and changes in the overall peak shapes) B' and A', in the positive scan observed during the first cycle (see curve a in this figure). The complementarity of peaks A and A', and B and B' was demonstrated by voltammetric scans performed over the region 1.0 - 2.4 V in one case and 1.6 - 3.0 V in the other (only the first of these is shown in curve c in this figure), affording definite proof that each of these set of peaks represents (following the first cycle) a unique redox process.

Coulometric analysis of the second and stable cycle over the entire voltage range, i.e. 0.9 to 3 V in curve b in this figure, revealed a total charge for the full discharge (ca. 0.3 C), which is only slightly higher than that obtained during full recharge (0.26 C), and in fairly good agreement with the amount of pyrite used in the cathode (ca. 0.1 mg) assuming a net four-electron process. The much higher overpotentials observed in the first full discharge (curve a) may be ascribed to kinetic hindrances associated with the intercalation of Li^+ into the pristine pyrite lattice.

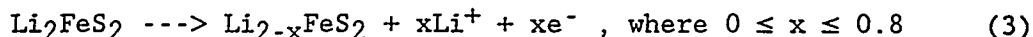
Although stepwise mechanisms, such as that proposed by Dahn et al.,^{2,3} would be consistent with the coulometric behavior observed during the second and subsequent cycles, an unambiguous assignment of voltammetric features can only be made on the basis of information derived from *in situ* spectroscopic and/or structural probes.

X-ray Absorption Fine Structure (XAFS)

In situ Fe K-edge XAFS data were acquired for FeS_2 electrodes in a single state of discharge or recharge in individual $\text{FeS}_2/\text{LiClO}_4/\text{Li}$ cells of identical construction, to avoid prolonged exposure of nominally sealed, air-sensitive components to the ambient atmosphere. Specifically, XAFS were collected for FeS_2 in a fresh cell (F), after the first full discharge (FD), after a half-recharge, immediately following full discharge (HR), and after a continuous full discharge and full recharge (FR). The voltammetric curves obtained in three of these independent measurements are shown in curves a through c in Fig. 4. As may have been expected based on the first voltammetric curve, the *in situ* XAFS of a fresh FeS_2 electrode polarized at 1.7 V was identical to that obtained for the same electrode at open circuit, i.e. 3 V.

Fig. 5 shows a series of *in situ* Fe K-edge XANES recorded for the cells denoted as F (solid line), FD (dot-dashed line), HR (dotted line), and FR (dashed line). As indicated, the full discharge of FeS_2 gives rise to profound spectral changes in this region (see dot-dash line in Fig. 5, and Panel A, Fig. 6), including sizable increases in intensity in the regions between 0 and 6 eV and 10 - 19 eV above Fe_{edge} . This trend is consistent with the formation of metallic iron, as evidenced by a comparison with the XANES of an Fe foil in transmission (see solid line in Panel A, Fig. 6), and, therefore, supports the assignment made by Dahn et al.^{2,3} on the basis of *in situ* XRD and ^{57}Fe MES. The *in situ* XANES for HR (dotted line) is

characterized by a well-defined pre-edge peak centered at 0.5 eV of a larger intensity than the rather flat feature found for (fresh) FeS₂ in the same energy range. Also noticeable is a slight shift of the edge position toward higher energies, as well as the appearance of an intense peak centered at about 15 eV compared to the *in situ* XANES of the fresh electrode (solid line). Somewhat surprising, however, are the striking similarities between the *in situ* XANES of HR (dotted line) and FR (dash line), which indicate that the electrochemical changes associated with the process shown in curve c, Fig. 3 do not involve the Fe center, but a sulfur-based redox couple, such as sulfide-disulfide, i.e. S₂²⁻ + 2e⁻ ---> 2S²⁻. This assignment is at variance with that proposed by Dahn et al.³, who inferred from *in situ* XRD data obtained for Li/Li₂FeS₂ batteries that the cycling between 1.45 and 2.45 V may be ascribed to the process



The series of k³χ(k) vs k spectra for the four specimens examined in the region 3 - 11.5 Å⁻¹ are shown curves a through d in Fig. 7, and the corresponding FT are displayed in Fig. 8. As was reported in a previous communication,⁵ the discharge of FeS₂ leads to a drastic decrease in the relative intensities of all distant shells, yielding FT curves with only a single shell attributed to nearest Fe-S interactions. The analysis of the inverse FT of this prominent shell EXAFS for HR and FR yielded Fe-S distances within experimental error identical to those of pyrite,¹¹ and, thus, incompatible with Fe-S bond lengths found in crystalline Li₂FeS₂, for which Fe-S₁ = 2.3737(7) Å and Fe-S₂ = 2.4126(15) Å.¹²

Insight into the possible nature of the iron sites in either HR or FR was obtained by identifying related materials with Fe-S bonds of about the same length. In fact, one of such materials is chalcopyrite, CuFeS₂,¹⁰ for which Fe²⁺ is surrounded by four sulfurs in a tetrahedral configuration at the same distance as that found in pyrite. A direct comparison between the XANES of CuFeS₂ and pyrite obtained in the transmission mode (see Panel B, Fig. 6) revealed three important differences (1) a more prominent pre edge peak; (2) a shift in the absorption edge toward higher energies (ca. 1 eV), and; (3) the occurrence of a peak at about 10 eV above the Fe edge. The same qualitative differences can be found between the XANES of HR (and also FR) and FeS₂, which suggests that the iron sites in both these species is also coordinated by four sulfur atoms in a tetrahedral-type environment.

Further insight into these redox processes is expected to be obtained from *in situ* S K-edge measurements. The energies involved in such experiments, however (ca. 2500 eV), are much lower than those involved in this work; hence, many of the cell materials and overall measurement strategy will have to be substantially modified to enable both the incident and fluorescent beams to penetrate through the cell structure.

ACKNOWLEDGEMENTS

This work was supported by the Department of Energy, Basic Energy Science. The NSLS is supported by the U.S. Department of Energy, Division of Material Sciences, and SSRL, is operated by the Department of Energy, Office of Basic Energy Sciences. M.R.A is supported by the U.S.DoE, Basic Energy Sciences-Chemical Sciences, under contract No. W-31-109-ENG-38.

REFERENCES

1. E. Peled, D. Golodnitsky, G. Ardel, J. Lang and Y. Lavi, *J. Power Sources*, 54, 496 (1995).
2. R. Fong, J. R. Dahn and C. H. W. Jones, *J. Electrochem. Soc.* 136, 3206 (1989).
3. R. Fong, C. H. W. Jones and J. R. Dahn, *J. Power Sources*, 26, 333 (1989).
4. S. K. Preto, Z. Tomczuk, S. von Winbusch and M. F. Roche, *J. Electrochem. Soc.*, 130, 264 (1983).
5. D. A. Tryk, S. Kim, Y. Hu, W. Xing, M. R. Antonio, V. Leger, G. Blomgren and D. A. Scherson, *J. Phys. Chem.* 99, 3732 (1995).
6. G. E. Blomgren, M. I. Lind, D. M. Radman, S. M. Rolland and H. Vourlis, (paper presented at *Portable by Design* Conference, Santa Clara, CA, February 1995).
7. a. Ichino, T.; Cahan, B. D.; Scherson, D. A. *J. Electrochem. Soc.* 138, L59 (1991).
b. Y. Gofer, R. Barbour, Y. Luo, D. A. Tryk, J. Jayne, G. S. Chottiner and D. A. Scherson, *J. Phys. Chem.* 99, 11739 (1995)
8. a. I. J. Pickering and G. N. George, *Inorg. Chem.* 34, 3142 (1995);
b. P. A. O'Day, J. J. Rehr, S. I. Zabinsky, G. E. Brown, Jr., *J. Am. Chem. Soc.*, 116, 2938 (1994).
9. a. J. J. Rehr, J. Mustre de Leon, S. I. Zabinsky, and R. C. Albers, *J. Am. Chem. Soc.* 113, 5135 (1991).
b. J. Mustre de Leon, J. J. Rehr, S. I. Zabinsky, and R. C. Albers, *Phys. Rev. B.*, 44, 4146 (1991).
10. J. Petiau, P. Saintavit and G. Calas, *Mat. Sci. and Eng.*, B1, 237 (1988)
11. S. L. Finklea III, L. C. Cathey and E. L. Amma, *Acta Cryst.* A32, 529 (1976).
12. R. J. Batchelor, F. W. B. Einstein and C. H. W. Jones, *Phys. Rev. B*, 37, 3699 (1988).

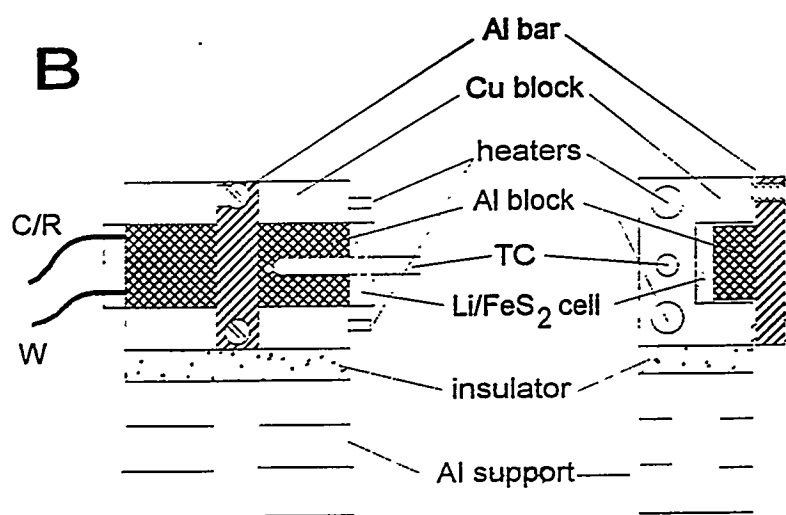
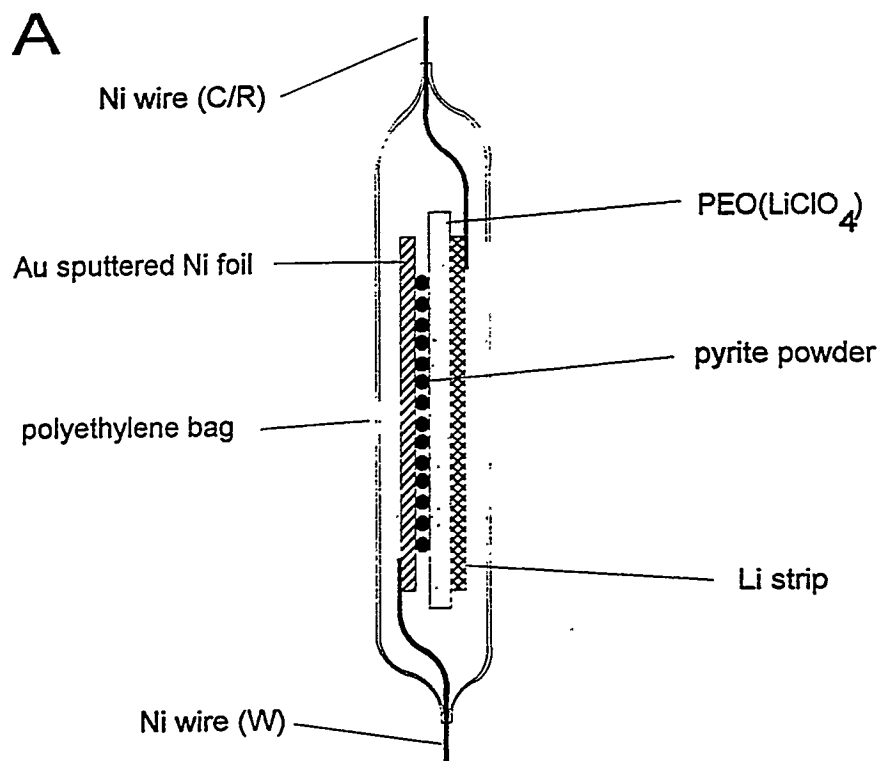


Fig. 1. Panel A. Schematic diagram of the Li/FeS₂ cell designed for *in situ* Fe-K-edge XAFS studies in the fluorescence mode. Panel B. Front and side views of the heater/assembly for electrochemical and *in situ* XAFS measurements.

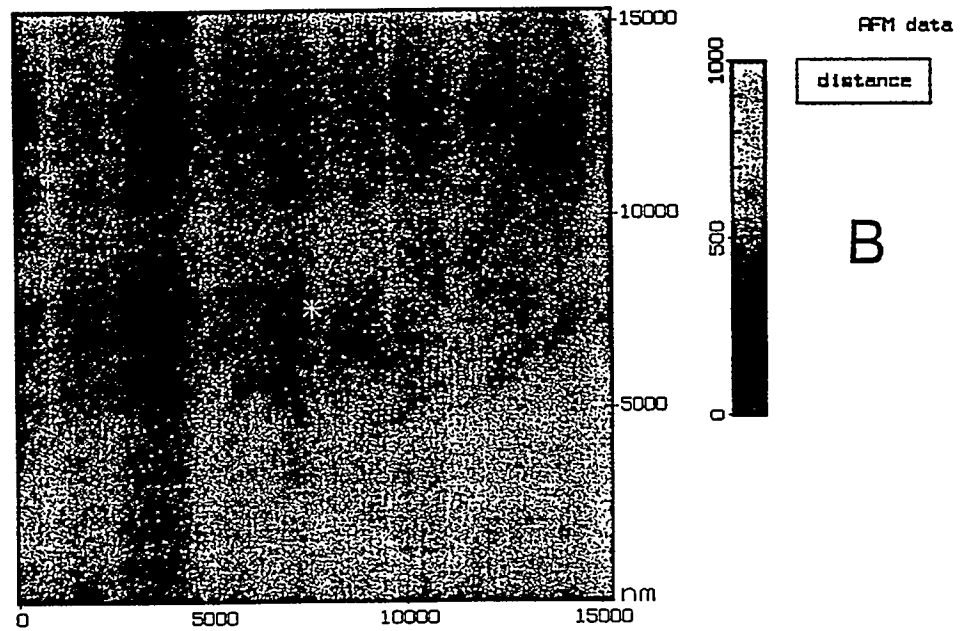
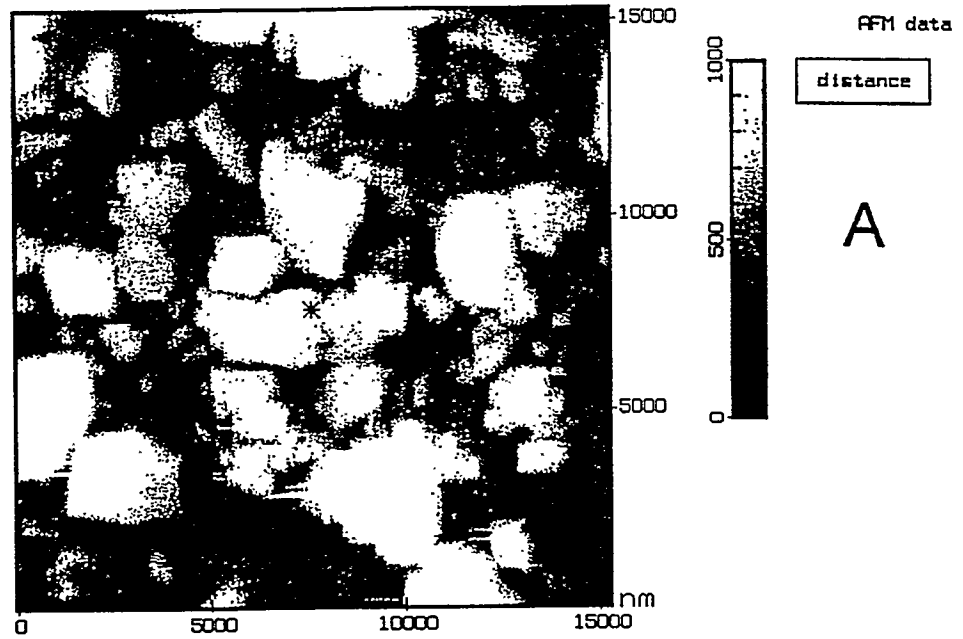


Fig. 2. Atomic force microscopy images of the dispersed pyrite cathode on the PEO(LiClO₄) film (Panel A) and of a bare PEO(LiClO₄) film (Panel B).

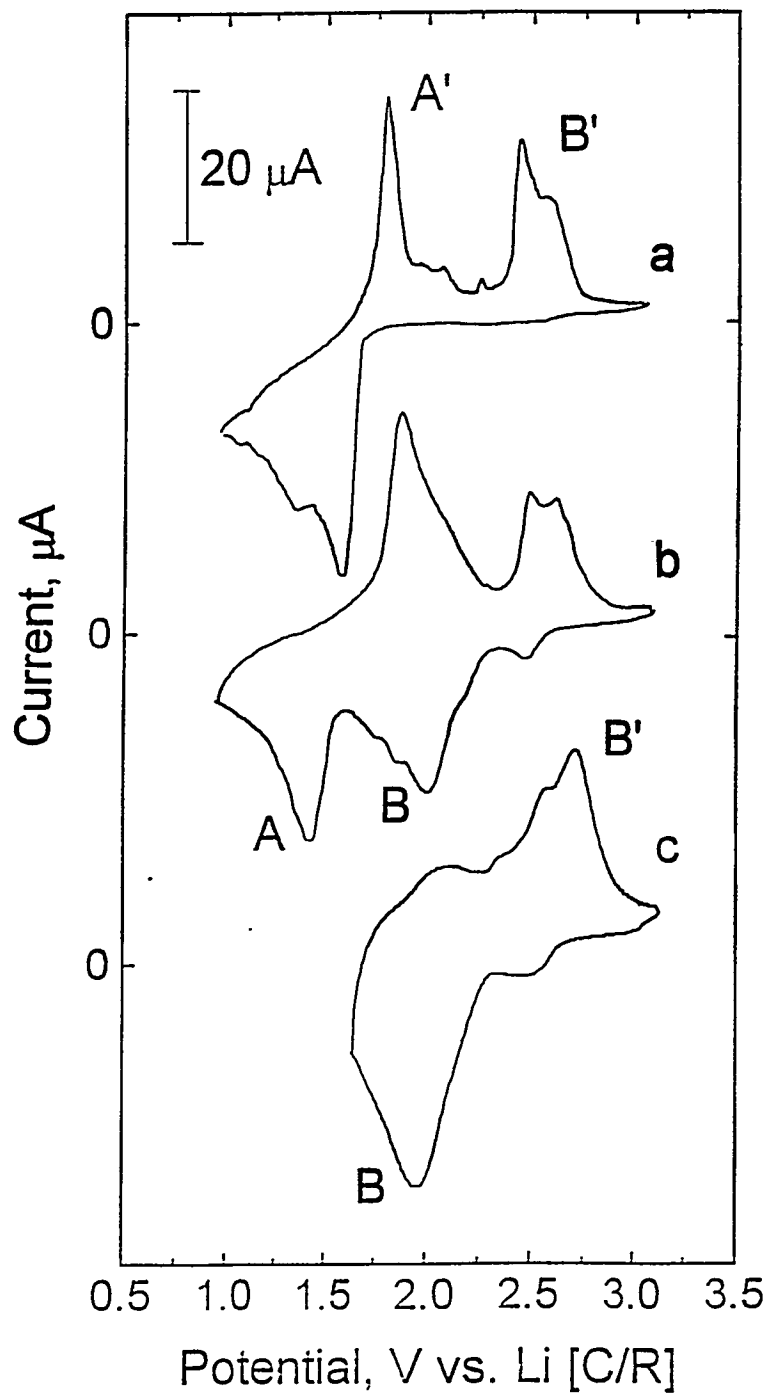


Fig. 3. First (curve a) and subsequent (curve b) cyclic voltammogram of a FeS_2 electrode recorded in a cell identical to that used in *in situ* XAFS experiments at 55°C initiated at the open circuit potential. Curve c shows a voltammetric scan in the region of the more positive redox process (see text). Scan rate: $70 \mu\text{V/s}$.

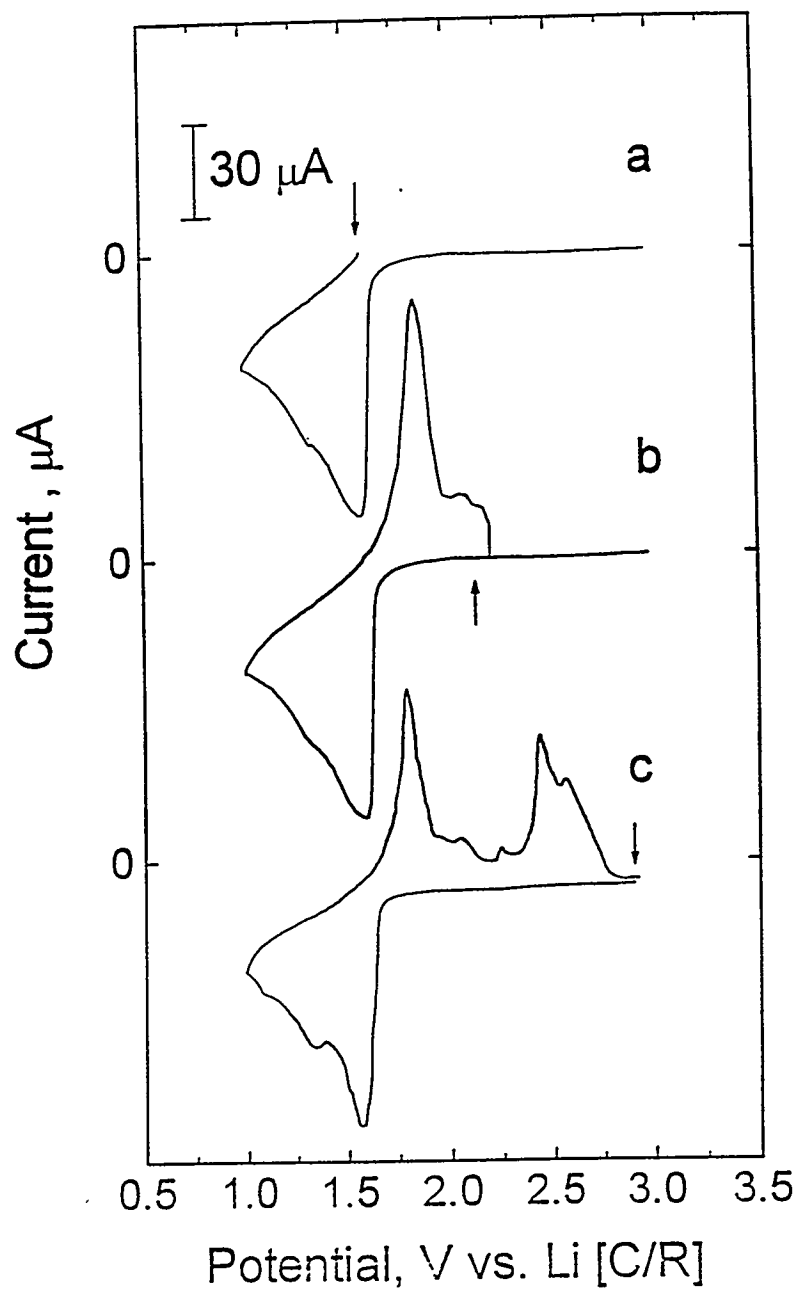


Fig. 4. Voltammetric curves obtained prior to the three independent *in situ* XAFS measurements. A. Fresh battery (F); B. fully discharged (FD); C. Half Recharged (HR); D. Fully recharged (FR).

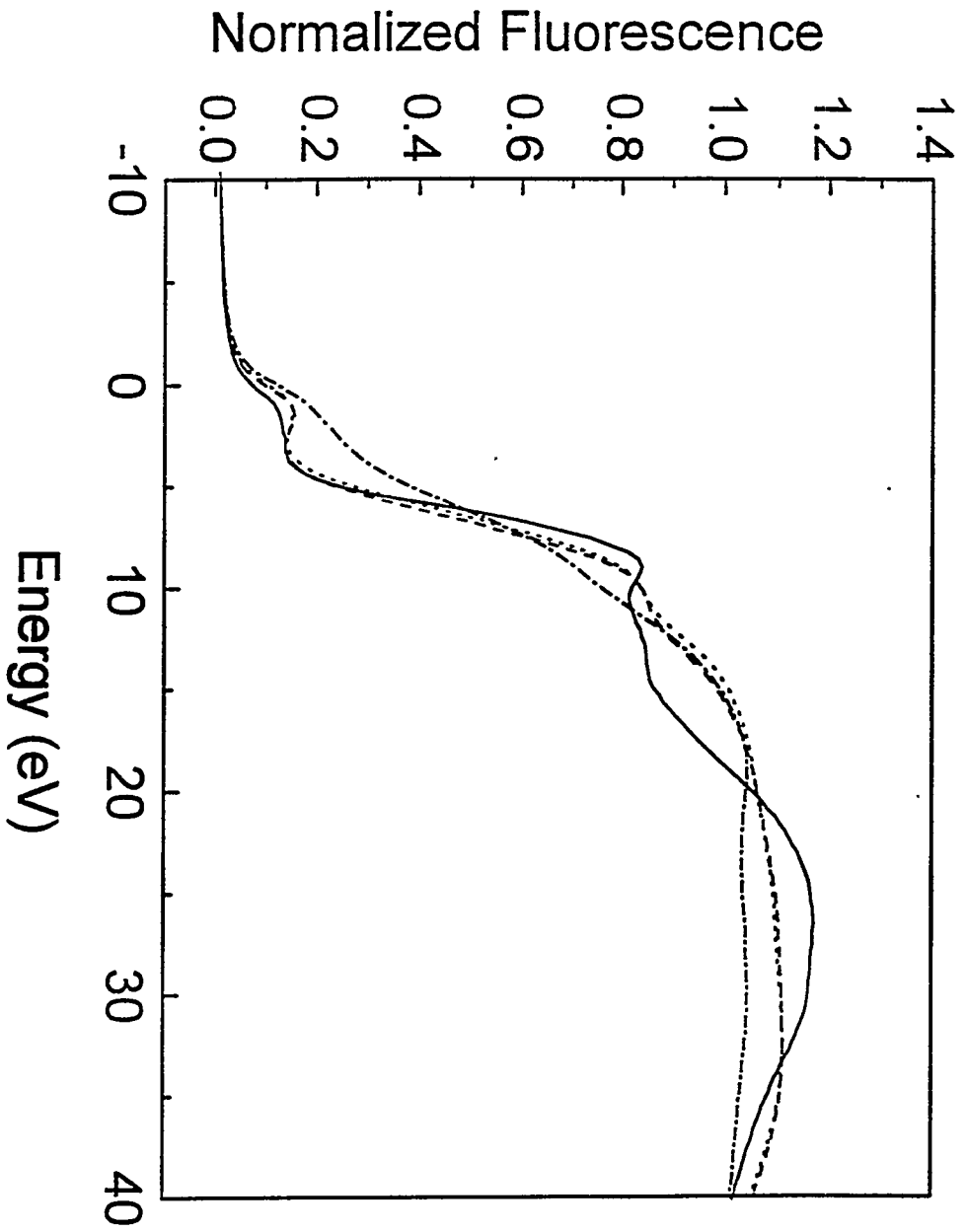


Fig. 5. Series of *in situ* Fe K-edge XANES recorded for the cells denoted as F, FD, HR, and FR in caption Fig. 5.

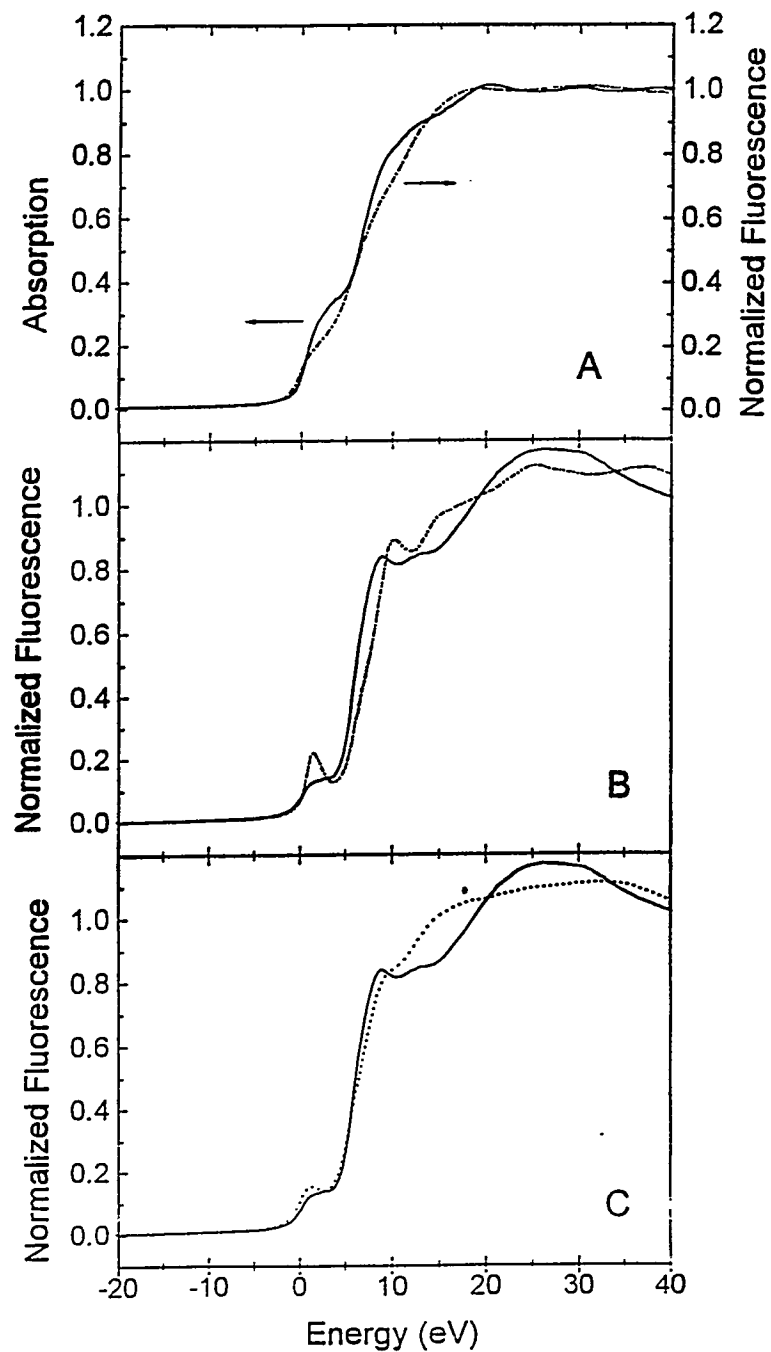


Fig. 6. Comparison between the *in situ* XANES of a fully discharged FeS_2/Li battery (FD in Fig. 5) and the *ex situ* XANES of metallic Fe obtained in the transmission mode (Panel A); *ex situ* XANES of FeS_2 and Cu_2FeS_2 (Panel B) and *in situ* XANES of F and HR in Fig. 5 (Panel C).

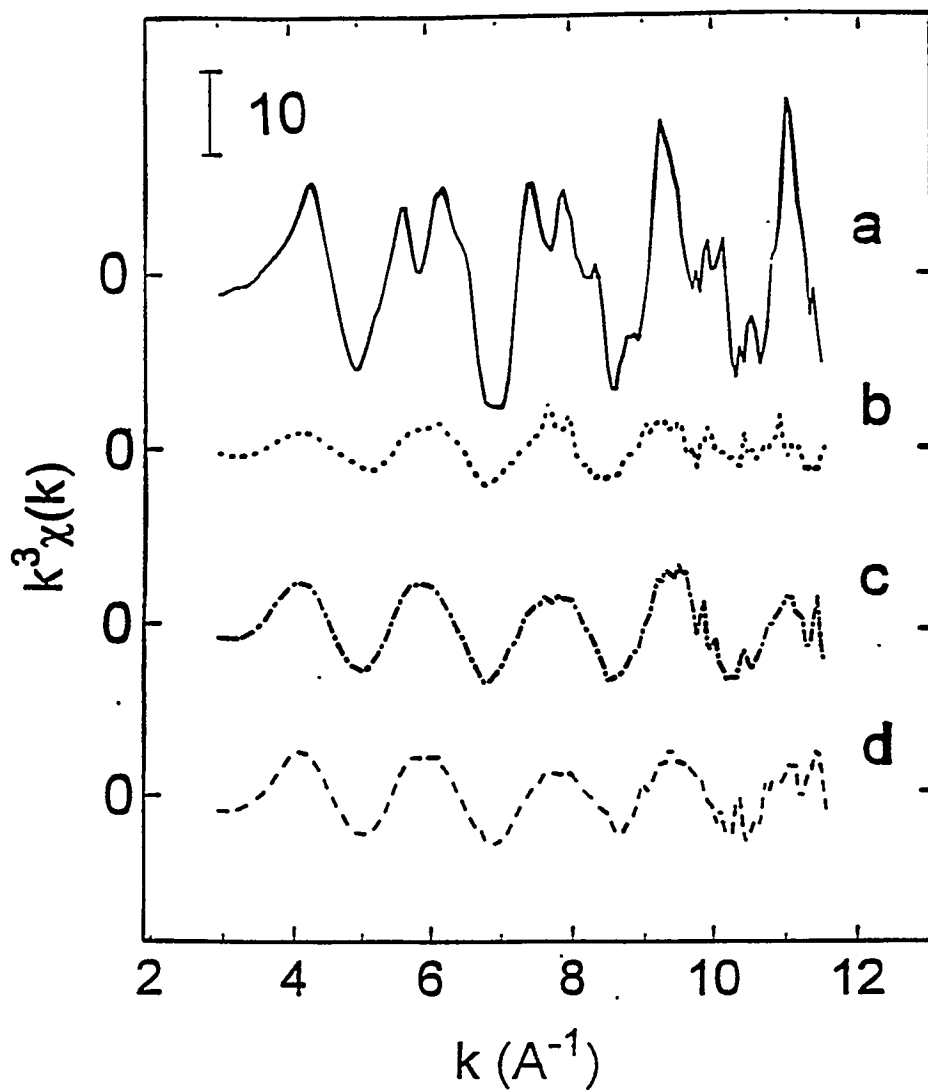


Fig. 7. Series of $k^3\chi(k)$ vs k spectra for the $\text{FeS}_2/(\text{PEO}, \text{LiClO}_4)/\text{Li}$ batteries specified in caption Fig. 4.

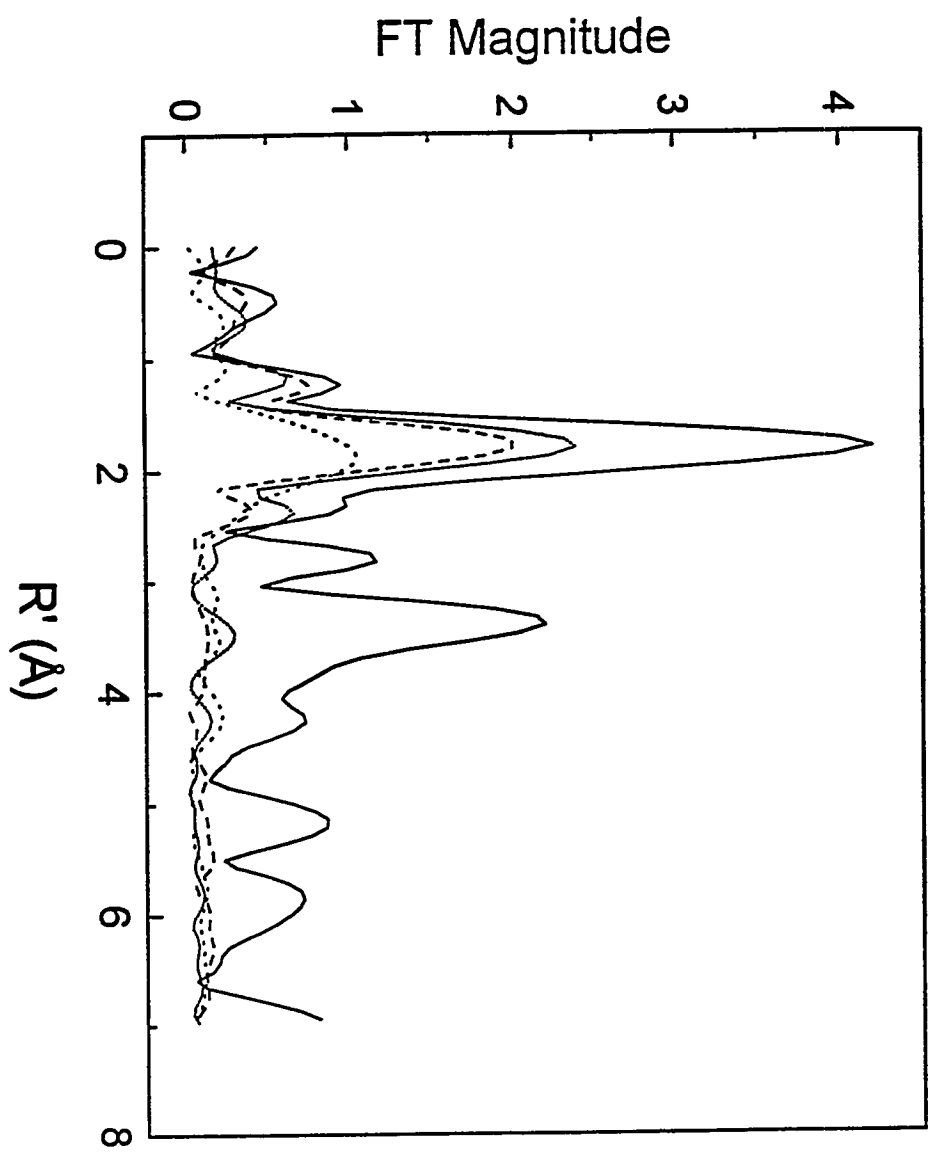


Fig. 8. Fourier transforms of the data in Fig. 7.